AIAA JOURNAL
Vol. 38, No. 11, November 2000

Higher-Order Buckling of Debonded (Delaminated) Sandwich Panels with Soft Core

Y. Frostig* and V. Sokolinsky†
Technion—Israel Institute of Technology, 32000 Haifa, Israel

Buckling behavior of sandwich panels with a transversely flexible core that are debonded at one of their face sheet–core interfaces is presented. The analytical model allows for a general configuration of the sandwich panel and nonrigid bond layers between the face sheets and core. The governing equations with the associated boundary and continuity conditions are derived through the variational principle of virtual work. Buckling response of the panels with inner and edge debondings (delaminations) is studied numerically. The effects of length and location of the delamination, face sheet rigidities, boundary conditions, and existence or inexistence of contact on the critical loads and buckling modes are presented. A comparison with experimental buckling modes is discussed, and conclusions are drawn.

I. Introduction

MODERN sandwich panels consist of two metallic or composite laminated face sheets bonded to a core that is made either of metallic or low-strength honeycomb or plastic foam. The ability of sandwich panels to resist loads depends heavily on the collaboration between the two face sheets, which is possible only due to the bond between the face sheets and the core. Loss of this bond through the entire length of the panel is catastrophic. However, debonding of one of the face sheets from the adjacent core at a certain region is a common imperfection that may occur during the manufacturing process or during the service life of the sandwich panel. The effects of this type of imperfection on the buckling behavior of sandwich panels are the focus of this paper.

Although the issue of debonding of the panel face sheets from the core is extremely important to the field of sandwich panels, few analytical and experimental studies of such structures exist. Kassapoglou[1] developed an analytical approach for investigation of laminated composite panels with an elliptical delamination within the laminate and subjected to compressive loads. He adapted it to a numerical and experimental study of sandwich panels with an incompressible core. Somers et al.[2] and Hwu and Hu[3] investigated the effects of a predetermined delamination, placed symmetrically with respect to the supports, on the buckling and the postbuckling behavior of laminated composite sandwich beams. The last two papers divided the sandwich beam into ordinary beam elements, one of which comprises the debonded portion of the face sheet, following the approach used by Simitses et al.[4] for the analysis of delaminated composite panels. Kim and Dharan[5] derived the relationships between the critical in-plane compressive load and the critical debond length for sandwich panels by combining the simplified linear buckling analysis with linear elastic fracture mechanics criteria. Lin et al.[6] proposed a two-dimensional continuous model of a delaminated face sheet of sandwich plates for local buckling using special fictitious normal and shear forces in the delaminated region. Kardomateas[7] considered the buckling of a delaminated sandwich panel by resorting to the panel-on-an-elastic-foundation approach. Zenkert[8] addressed experimentally the case of interface debonding (delamination) in sandwich beams and suggested a criteria based on a damage tolerance approach.

All of the discussed papers assume that the overall and the localized modes of the buckling response are uncoupled. The term localized mode here refers to a deformation pattern that is confined to some zone along the panel and affects the two face sheets, whereas the local mode refers to a deformation pattern that affects the face sheets, but extends through the entire length of the panel, such as wrinkling.

Recently, Avery et al.[9] presented an extensive experimental study on the buckling of delaminated sandwich panels when subjected to in-plane loads. Although the delamination is located only at one of the face sheet–core interfaces, the experimental study reveals that the buckling mode affects the two face sheets rather than being limited to the debonded face sheet only. It means that the behavior of delaminated sandwich panels is absolutely different from that of composite laminated panels with thin-film delamination.[4] Furthermore, such phenomena as mode interaction and mode shift from one buckling mode to another have been observed in the experiments of Avery et al.[9] These experimental results contradict the usual approach which assumes that the stability of the debonded panel can be analyzed by considering the buckling of a thin delaminated composite face sheet resting on an elastic foundation in isolation from the other face sheet.

The mode decoupling approach has been a predominant tool for the analysis of sandwich structures with incompressible (stiff) core types in the last few decades.[10–13] Following this approach, the sandwich panel is replaced by an equivalent transversely incompressible panel with a transverse shear rigidity for the overall buckling analysis, whereas the beam-on-an-elastic foundation model is used to determine the local buckling behavior. As a result, the interaction between the overall and the local modes of the buckling response, as well as any collaboration between the two face sheets, is ignored for local (localized) buckling. Moreover, the use of the presumed buckling modes reduces substantially the generality of the analysis and leads in many cases to misleading results and in some cases even to incorrect results. The experimental study by Avery et al.[9] reveals that the application of the mode decoupling approach for the delaminated panels, even with a stiff core, in most of the cases is unjustified. It is even more misleading whenever a compressible (soft) type of the core is considered because a collaboration between the two face sheets always occurs, the overall and local (localized) buckling modes essentially interact, and a shifting between the modes may accompany the buckling response.

Frostig et al.[14] and Frostig and Baruch[15] presented a rigorous higher-order theory for sandwich panels (HSAPT) of a general configuration with a transversely flexible core. The theory does not resort to the mode decoupling approach along with presumed buckling patterns but provides a general analysis accounting for a mode interaction phenomenon. Moreover, the HSAPT enables one to treat the real supporting systems, such as different types of boundary conditions (supports) at the upper and the lower face sheets at the same edge. The assumptions used are as follows: The panel behavior is linear elastic, the face sheets are modeled by ordinary panels (with

Received 9 September 1999; revision received 21 April 2000; accepted for publication 28 April 2000.

*Associate Professor, Department of Civil Engineering.
†Ph.D. Student, Department of Civil Engineering; currently Research Scholar, Center for Composite Materials, University of Southern California, Vivian Hall of Engineering 402, Los Angeles, CA 90089-0241.

negligible shear strains) that follow Euler–Bernoulli assumptions and are subjected to the intermediate class of deformations,[16] and the core layer is considered as a two-dimensional elastic medium with small deformations, where the height of the soft core may change under loading, whereas its cross-sectional plane does not remain plane. The longitudinal (in-plane) stresses are neglected as a result of the very low longitudinal rigidity of the core layer with respect to the rigidities of the face sheets, which is similar to the assumption used for an antiplane core.[11] The interface layers are assumed to resist shear and vertical normal (peeling) stresses and to provide a full bond between the core and face sheets.

Thomsen and Frostig[17] presented an experimental photoelastic verification of the HSAPT for the stress field induced by the application of highly concentrated external loads and point supports. HSAPT has been applied by Frostig[18] to analyze the stress concentration involved in bending behavior of delaminated sandwich panels with a soft core.

This paper deals with the buckling of debonded (delaminated) sandwich panels, where the debonded zone is located at one of the face sheet–core interfaces. The approach presented is based on the HSAPT, as well as on the numerical procedure used for the linear buckling analysis of the perfect sandwich panels by Sokolinsky and Frostig.[19] The analytical model allowing for nonrigid bond layers between the face sheets and core is outlined first. Then the nonlinear governing equations with appropriate boundary and continuity conditions are derived through the variational principle of virtual work. A numerical study that determines the influence of the delamination length and its location through the span of the panel, as well as of contact between the layers in the debonded region, on the critical loads and buckling modes is presented next. Qualitative comparisons with the experiments of Avery et al.[9] are discussed and conclusions are drawn.

II. Mathematical Formulation

The analytical model presented is an extension of HSAPT[15] to the nonrigid bond layers between the face sheets and core (Fig. 1). The nonrigid layers consist of equivalent horizontal and vertical springs that simulate a slip between the face sheets and core, as well as contact effects, respectively (Fig. 1c). The springs are linear and can resist compression as well as tension. It is assumed that a through-the-width debonding (delamination) between one of the face sheets and the core has a length l_d and its center is at a distance L_d from the left edge of the panel (Fig. 1a). Analytically, the delamination is achieved by means of a reduction of the horizontal spring coefficient to a very low value. If the contact is ignored, then the vertical spring coefficient approaches zero at the debonded zone.

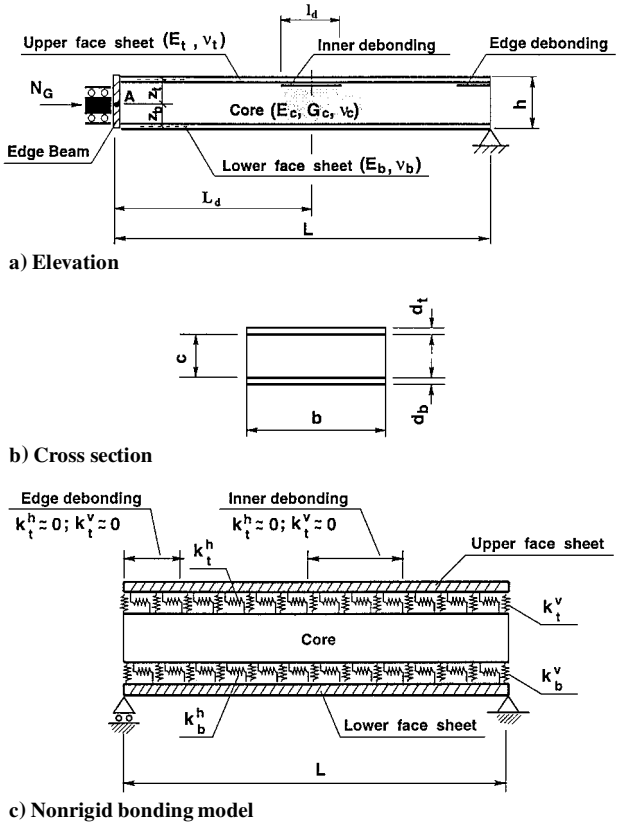

Fig. 1 Sandwich panel layout.

A. Nonlinear Field Equations

The derivation is based on the principle of virtual work, which requires that the external virtual work δW must equal the internal virtual work δU. The internal virtual work is

$$\delta U = \iiint_{V_t} \sigma_{xxt}\delta\varepsilon_{xxt}\,\mathrm{d}V + \iiint_{V_b} \sigma_{xxb}\delta\varepsilon_{xxb}\,\mathrm{d}V + \iiint_{V_c} \tau\delta\gamma\,\mathrm{d}V + \iiint_{V_c} \sigma_{zz}\delta\varepsilon_{zz}\,\mathrm{d}V + \int_0^L \left[F_t^h\delta\Delta u_t + F_b^h\delta\Delta u_b + F_t^v\delta\Delta w_t + F_b^v\delta\Delta w_b\right]\mathrm{d}x \quad (1)$$

where V_t, V_b, and V_c are the volumes of the upper and the lower face sheets and the volume of the core, respectively (Fig. 2a); $\mathrm{d}V$ is the elementary volume; L is the length of the panel (Fig. 1a); $\mathrm{d}x$ is the elementary length, where by x implies any of three axes, x_t, x_b, or x_c (Fig. 2a); σ_{xxt} and ε_{xxt} and σ_{xxb} and ε_{xxb} are the longitudinal normal stresses and strains in the upper and the lower face sheets, respectively; τ and γ are the shear stresses and strains, and σ_{zz} and ε_{zz} are the vertical normal stresses and strains in the core layer, respectively. F_t^h and F_b^h and F_t^v and F_b^v are the horizontal and the vertical spring reactions per unit length at the upper and the lower interfaces, respectively (Fig. 2b) and Δu_t and Δw_t and Δu_b and Δw_b are the relative displacements in the horizontal and the vertical directions of the face sheets and the core at the upper and the lower face sheet–core interfaces, respectively (Fig. 2c).

The spring reactions per unit length in the horizontal direction are defined as

$$F_t^h = bk_t^h\Delta u_t \quad (2)$$

$$F_b^h = bk_b^h\Delta u_b \quad (3)$$

and those in the vertical direction are

$$F_t^v = bk_t^v\Delta w_t \quad (4)$$

$$F_b^v = bk_b^v\Delta w_b \quad (5)$$

where b is the width of the panel cross section (Fig. 1b), k_t^h and k_b^h are the spring coefficients in the horizontal direction and k_t^v and k_b^v are the spring coefficients in the vertical direction at the top and the bottom interfaces, respectively.

The relative displacements of the interface springs in the horizontal and vertical directions (Figs. 1c, 2a, and 2c) are

$$\Delta u_t = u_c(B) - u_t(A) = u_c(x,0) - u_{0t}(x) + (d_t/2)w_{t,x}(x) \quad (6)$$

$$\Delta u_b = u_b(C) - u_c(D) = u_{0b}(x) + (d_b/2)w_{b,x}(x) - u_c(x,c) \quad (7)$$

$$\Delta w_t = w_c(B) - w_t(A) = w_c(x,0) - w_t(x) \quad (8)$$

$$\Delta w_b = w_b(C) - w_c(D) = w_b(x) - w_c(x,c) \quad (9)$$

where u_{0t} and u_{0b} and w_t and w_b are the longitudinal and the vertical displacements of the centroid line of the upper and the lower face sheets, respectively; $w_{t,x}$ and $w_{b,x}$ are the rotations of the upper and the lower face sheets, respectively; subscript x denotes the derivative with respect to x; u_c and w_c are the horizontal and the vertical displacements of the core, respectively; d_t and d_b are the thicknesses of the upper and the lower face sheets, respectively (Figs. 1b and 2a); $u_t(A)$ and $w_t(A)$ and $u_b(C)$ and $w_b(C)$ are the longitudinal and the vertical displacements of points A and C of the upper and the lower

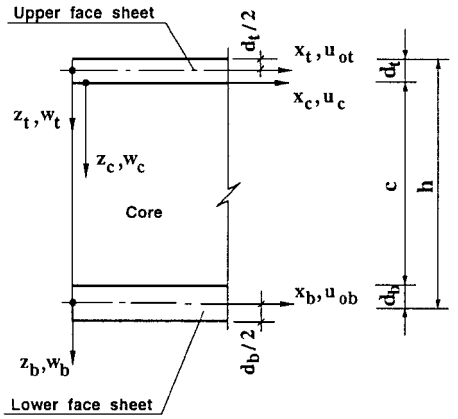

a) Geometry

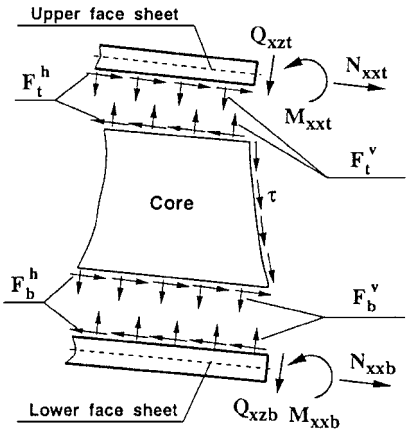

b) Internal stresses and stress resultants

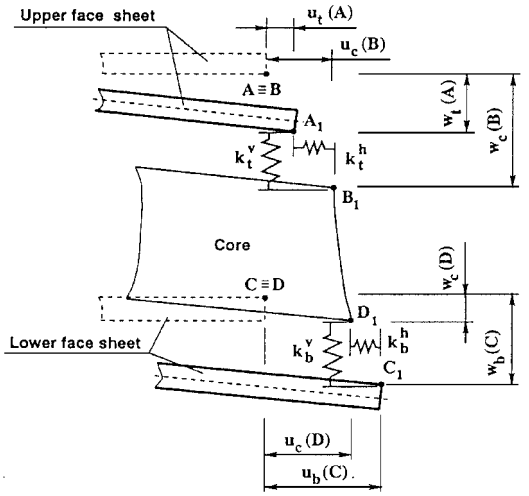

c) Cross-sectional deformation

Fig. 2 Sandwich panel conventions.

face sheets, respectively (Fig. 2c); and $u_c(B)$ and $w_c(B)$ and $u_c(D)$ and $w_c(D)$ are the longitudinal and the vertical displacements of points B and D of the upper and the lower edges of the core, respectively. Notice that Euler–Bernoulli assumptions have been used to represent the displacements of the face sheets. It can be seen from Eqs. (6–9) that the formulation presented is a two-dimensional one.

The external virtual work is

$$\delta W = \int_0^L (q_t \delta w_t + q_b \delta w_b + n_t \delta u_{0t} + n_b \delta u_{0b} + m_t \delta w_{t,x} + m_b \delta w_{b,x})\,dx + \sum_{j=1}^{N_c} \int_0^L (P_{tj} \delta w_t + P_{bj} \delta w_b + N_{tj} \delta u_{0t} + N_{bj} \delta u_{0b} + M_{tj} \delta w_{t,x} + M_{bj} \delta w_{b,x}) \delta_D(x - x_j)\,dx \tag{10}$$

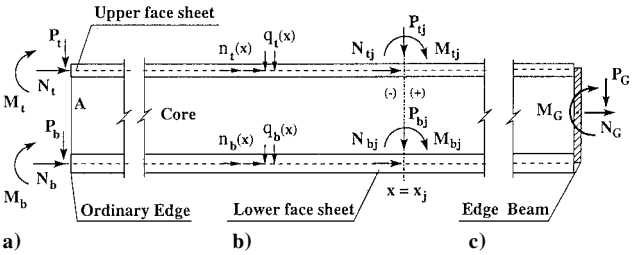

Fig. 3 External loads exerted on panel a) at an edge beam support; b) within the span, distributed and concentrated; and c) at an ordinary edge.

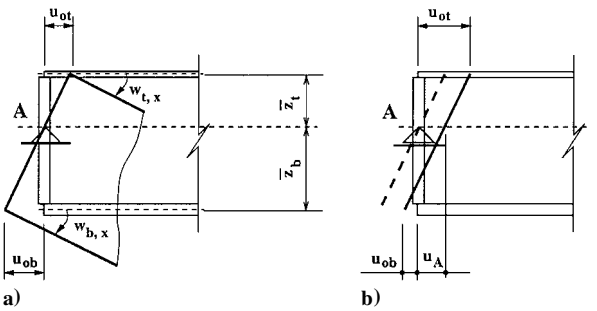

Fig. 4 Edge beam displacement patterns at a) hinge support and b) roller support.

where (Figs. 3a and 3b) q_t and q_b and n_t and n_b are the distributed vertical and horizontal external loads and m_t and m_b are the distributed bending moments exerted on the upper and the lower face sheets, respectively; P_{tj} and P_{bj} and N_{tj} and N_{bj} are the concentrated line vertical and horizontal loads; M_{tj} and M_{bj} are the concentrated line moments applied at the upper and the lower face sheets, respectively, at $x = x_j$. N_c is a number of concentrated loads and $\delta_D(x - x_j)$ is the Dirac delta function.

When a rigid diaphragm, denoted by edge beam (see Figs. 1a and 3c) is attached to the edge of the sandwich panel, the expression for the external virtual work in Eq. (10) must be supplemented with

$$\delta V_{BC} = -(N_G \delta u_A + M_G \delta w_{A,x} + P_G \delta w_A) \tag{11}$$

where u_A, w_A, and $w_{A,x}$ are the displacements in the horizontal and the vertical directions and the rotation, respectively, at the supporting point A (Fig. 3c). N_G, P_G, and M_G are the global external concentrated forces in the horizontal and vertical directions and the global concentrated moment at the point A (Figs. 3c and 4). Note that, in the case of the edge beam, the external loads are applied to the edge of the panel at the point A in the global sense as opposed to the ordinary case, where the external loads are applied directly to the various face sheets.

The global quantities describing the kinematics of the edge beam are given by

$$w_A = w_t \tag{12}$$

$$w_{A,x} = w_{t,x} \tag{13}$$

$$u_A = \frac{u_{0t}\bar{z}_b + u_{0b}\bar{z}_t}{\bar{z}_t + \bar{z}_b} \tag{14}$$

where $\bar{z}_t$ and $\bar{z}_b$ are the distances from the support point A to the centroids of the upper and the lower face sheets, respectively (Fig. 4a).

The kinematic relations used for the upper and lower face sheets are those of the intermediate class of deformations[16]:

$$\varepsilon_{xxi} = u_{0i,x} + \tfrac{1}{2} w_{i,x}^2 - z_i w_{i,xxx}, \qquad i = t, b \tag{15}$$

where z_i $(i = t, b)$ is the vertical coordinate of each face sheet measured downward from its centerline (Fig. 2a).

The stress–displacement relationships for the core assuming small deformations are

$$\gamma = u_{c,z_c} + w_{c,x} \tag{16}$$

$$\varepsilon_{zz} = w_{c,z_c} \tag{17}$$

where z_c is the vertical coordinate of the core measured downward from the upper face sheet–core interface (Fig. 2a).

The field equations, as well as the associated boundary and continuity conditions, for the sandwich panel with the nonrigid layers are derived using Eqs. (1) and (10), with the kinematic relationships in Eq. (15) and the compatibility conditions in Eqs. (6–9). After some algebraic manipulations, the following set of field equations is determined:

$$N_{xxt,x} + F_t^h + n_t = 0 \tag{18}$$

$$N_{xxb,x} - F_b^h + n_b = 0 \tag{19}$$

$$M_{xxt,xx} + (N_{xxt}w_{t,x})_{,x} + F_{t,x}^h d_t/2 + F_t^v + q_t - m_{t,x} = 0 \tag{20}$$

$$M_{xxb,xx} + (N_{xxb}w_{b,x})_{,x} + F_{b,x}^h d_b/2 - F_b^v + q_b - m_{b,x} = 0 \tag{21}$$

$$\tau_{,x} + \sigma_{zz,z_c} = 0 \tag{22}$$

$$\tau_{,z_c} = 0 \tag{23}$$

$$F_t^h - b\tau(x, z_c = 0) = 0 \tag{24}$$

$$F_b^h - b\tau(x, z_c = c) = 0 \tag{25}$$

$$F_t^v - b\sigma_{zz}(x, z_c = 0) = 0 \tag{26}$$

$$F_b^v - b\sigma_{zz}(x, z_c = c) = 0 \tag{27}$$

where the stress resultants in terms of the longitudinal normal stresses σ_{xxi}, $i = t, b$, are defined as

$$N_{xxi} = b\int_{-d_i/2}^{d_i/2} \sigma_{xxi}\,\mathrm{d}z_i, \qquad M_{xxi} = b\int_{-d_i/2}^{d_i/2} \sigma_{xxi} z_i\,\mathrm{d}z_i \tag{28}$$

and $\mathrm{d}z_i$ is the elementary length of each face sheet in the vertical direction.

Notice that Eq. (23) implies that τ must be constant through the height of the core; in other words, τ is a function of the longitudinal coordinate only and, therefore,

$$\tau(x, z_c = 0) = \tau(x, z_c = c) = \tau(x) \tag{29}$$

The boundary conditions at the left ($x = 0$) and the right ($x = L$) edges of the panel resulting from the variational procedure are given for each face sheet and the core separately. Hence, for the ordinary edge (see Fig. 3a), the boundary conditions at the face sheets, $i = t, b$, are

$$\xi N_{xxi} = N_i \qquad \text{or} \qquad u_{0i} = \bar{u}_{0i} \tag{30}$$

$$\xi M_{xxi} = -M_i \qquad \text{or} \qquad w_{i,x} = \bar{w}_{i,x} \tag{31}$$

$$\xi\left[M_{xxi,x} + N_{xxi}w_{i,x} + F_i^h(d_i/2) - m_i\right] = P_i \qquad \text{or} \qquad w_i = \bar{w}_i \tag{32}$$

where $\xi = -1$ at $x = 0$ and $\xi = 1$ at $x = L$. N_i and P_i are the external horizontal and vertical loads and M_i is the bending moment applied at the ends of each face sheet, $i = t, b$, respectively; $\bar{u}_{0i}$, $\bar{w}_i$, and $\bar{w}_{i,x}$ are the prescribed longitudinal and vertical displacements and rotations of each face sheet, $i = t, b$, respectively. The boundary conditions at any point through the height of the core at $x = 0$ and L are $\tau = 0$ or the fulfillment of either of the two conditions

$$\int_0^c w_c(x, z_c)\,\mathrm{d}z_c = c\bar{w}_c(x), \qquad w_c(x, z_c) = \bar{w}_c(x, z_c) \tag{33}$$

where the constant $\bar{w}_c(x)$ is the prescribed vertical displacement at any point through the height of the core and $\bar{w}_c(x, z_c)$ is the prescribed displacement pattern of the core edge.

Alternatively, when the edge beam is attached to the edge of the sandwich panel (Fig. 3c), the boundary conditions are

$$w_t = w_b \tag{34}$$

$$w_{t,x} = w_{b,x} \tag{35}$$

$$w_{t,x} = \frac{u_{0t} - u_{0b}}{\bar{z}_t + \bar{z}_b} \tag{36}$$

$$\xi(N_{xxt} + N_{xxb}) = N_G \qquad \text{or} \qquad u_A = u_G \tag{37}$$

$$\xi(\bar{z}_t N_{xxt} - \bar{z}_b N_{xxb} - M_{xxt} - M_{xxb}) = M_G \qquad \text{or} \qquad w_{A,x} = w_{G,x} \tag{38}$$

$$\xi\Big[M_{xxt,x} + N_{xxt}w_{t,x} + M_{xxb,x} + N_{xxb}w_{b,x} + bc\tau + \left(F_t^h d_t + F_b^h d_b\right)/2\Big] = P_G \qquad \text{or} \qquad w_A = w_G \tag{39}$$

$$\tau_{,x} = 0 \tag{40}$$

where u_G, w_G, and $w_{G,x}$ are the specified values of the deformations at the supporting point A. Notice that Eqs. (34–36) are independent of the support type at the point A (Fig. 4). Some additional notes concerning the edge beams can be found in Ref. 20.

The continuity conditions at any $x = x_j$ along the span of the panel (Fig. 3b) include three geometrical and three natural conditions for each face sheet, as well as one geometrical and one natural condition for the core. Therefore, the continuity conditions at the face sheets, $i = t, b$, are given by

$$u_{0i}^{(-)} = u_{0i}^{(+)} \tag{41}$$

$$w_i^{(-)} = w_i^{(+)} \tag{42}$$

$$w_{i,x}^{(-)} = w_{i,x}^{(+)} \tag{43}$$

$$N_{xxi}^{(-)} - N_{xxi}^{(+)} = N_{ij} \tag{44}$$

$$-M_{xxi}^{(-)} + M_{xxi}^{(+)} = M_{ij} \tag{45}$$

$$M_{xxi,x}^{(-)} + N_{xxi}^{(-)}w_{i,x}^{(-)} + F_i^{h(-)}\left(d_i^{(-)}/2\right) - m_i^{(-)} - M_{xxi,x}^{(+)} - N_{xxi}^{(+)}w_{i,x}^{(+)} - F_i^{h(+)}\left(d_i^{(+)}/2\right) + m_i^{(+)} = P_{ij} \tag{46}$$

where the signs $(-)$ and $(+)$ are left and right of $x = x_j$. N_{ij}, P_{ij}, and M_{ij} are the external concentrated line loads in the longitudinal and the vertical directions and the concentrated line moment exerted at the upper and the lower face sheets, respectively, at $x = x_j$.

The continuity conditions at any point through the height of the core are

$$\tau^{(-)} = \tau^{(+)} \tag{47}$$

$$w_c^{(-)}(x_c = x_j, z_c) = w_c^{(+)}(x_c = x_j, z_c)$$

or

$$\int_0^c w_c^{(-)}(x_c = x_j, z_c)\,\mathrm{d}z_c = \int_0^c w_c^{(+)}(x_c = x_j, z_c)\,\mathrm{d}z_c \tag{48}$$

B. Stress and Displacement Fields of the Core

The uncoupled set of partial differential equations [Eqs. (22) and (23)] permits the determination of the stress and deformation fields in the core in terms of its shear stress, as well as longitudinal and vertical displacements of the face sheets.

The constitutive relationships for the core layer are

$$\tau = G_c\gamma \tag{49}$$

$$\sigma_{zz} = E_c w_{c,z_c} \tag{50}$$

where G_c and E_c are the shear and elastic moduli of the core. On the other hand, the transverse normal stresses using Eqs. (22) and (29) appear as

$$\sigma_{zz} = -\tau_{,x}z + \sigma_{zz}(x, z_c = 0) \tag{51}$$

The vertical deformation $w_c(x, z_c)$ is determined with the aid of Eqs. (50) and (51) through integration with respect to z_c and use of the compatibility condition in the vertical direction at the upper interface [Eq. (8)], as well as of Eq. (4). It is

$$w_c(x, z_c) = -\left(c^2/2E_c\right)\tau_{,x} + \left(c/E_c + 1/k_t^v\right)\sigma_{zz}(x, z_c = 0) + w_t \tag{52}$$

The normal stresses at the upper interface are determined, by the use of Eq. (51) along with the compatibility condition at the lower interface [Eq. (9)] and Eqs. (52) and (5), as

$$\sigma_{zz}(x, z_c = 0) = \frac{w_b - w_t + c\left[1/k_b^v + c/(2E_c)\right]\tau_{,x}}{c/E_c + 1/k_t^v + 1/k_b^v} \tag{53}$$

Hence, Eq. (51) becomes

$$\sigma_{zz}(x, z_c) = (1/\beta)(w_b - w_t) + (\alpha/\beta - z_c)\tau_{,x} \tag{54}$$

where $\alpha = c[c/(2Ec) + 1/k_b^v]$ and $\beta = c/E_c + 1/k_t^v + 1/k_b^v$. Note the linear dependency of the normal stresses in the core on the vertical coordinate z_c.

The vertical displacements of the core are derived through substitution of Eq. (53) into Eq. (52):

$$w_c(x, z_c) = \left(\alpha a_1/\beta - z_c^2/2E_c\right)\tau_{,x} + (a_1/\beta)w_b + [1 - (a_1/\beta)]w_t \tag{55}$$

where $a_1 = z_c/E_c + 1/k_t^v$. It can be seen from Eq. (55) that the vertical displacement in the core varies parabolically with the coordinate z_c.

The longitudinal displacements in the core layer are determined using the kinematic relationship [Eq. (16)], the constitutive law [Eq. (49)], and the vertical displacements of the core [Eq. (55)]. Integration with respect to x and application of the compatibility condition in the longitudinal direction at the upper interface [Eq. (6)] yield

$$u_c(x, z_c) = \left(\frac{z_c}{G_c} + \frac{1}{k_t^h}\right)\tau - z_c\left(\frac{\alpha a_2}{\beta} - \frac{z_c^2}{6E_c}\right)\tau_{,xx} - \frac{z_c a_2}{\beta}w_{b,x} + \left[z_c\left(\frac{a_2}{\beta} - 1\right) - \frac{d_t}{2}\right]w_{t,x} + u_{0t} \tag{56}$$

where $a_2 = z_c/(2E_c) + 1/k_t^v$. Hence, the longitudinal displacement distribution through the thickness of the core is represented by a polynomial of a cubic order in z_c.

Notice that when the spring coefficients approach infinity, Eqs. (54–56) reduce to the stress and deformation fields that have been derived by Frostig et al.[14] for the perfect sandwich panel.

C. Governing Equations

The governing differential equations for the sandwich panel with the nonrigid layers are formulated in terms of the following five unknowns: the horizontal displacements u_{0t} and u_{0b} and the vertical displacements w_t and w_b of the face sheets and the shear stress in the core τ.

The constitutive relations for the face sheets are those of a composite layer with symmetric layup and they are, where $i = t, b$,

$$N_{xxi} = A_{11i}\varepsilon_{xxi} \tag{57}$$

$$M_{xxi} = -D_{11i}w_{i,xx} \tag{58}$$

where A_{11i} and D_{11i} are the equivalent axial and flexural rigidities of the face sheets, respectively, defined by

$$(A_{11i}, D_{11i}) = b\int_{-d_i/2}^{d_i/2} Q_{11i}^{(k)}\left(1, z_i^2\right)\mathrm{d}z_i \tag{59}$$

where $Q_{11i}^{(k)}$ are the reduced stiffness coefficients of kth ply of the laminate[21] and z_i is the transverse direction of the face sheet Cartesian coordinates x and z_i, where x lies on the centroid line of each face sheet (Fig. 2a). Notice that Eqs. (57–59) can be applied to a narrow or a wide beam and that the term panel here applies to both cases.

Elimination of the horizontal and vertical spring reactions from the formulation with the aid of Eqs. (24–27) reduces the set of the field equations to four equations in five unknowns [Eqs. (22) and (23) have been used to solve for the core stress and deformation fields]. The additional equation is derived using the compatibility condition in the horizontal direction at the lower face sheet–core interface [Eq. (7)].

Thus, substitution of the constitutive and kinematic relationships for the face sheets, as well as Eq. (54) for the peeling stresses, into the field equations [Eqs. (18–21)] after some algebraic manipulations yields

$$A_{11t}(u_{0t,xx} + w_{t,x}w_{t,xx}) + \tau b = 0 \tag{60}$$

$$A_{11b}(u_{0b,xx} + w_{b,x}w_{b,xx}) - \tau b = 0 \tag{61}$$

$$-D_{11t}w_{t,xxxx} + A_{11t}\left(u_{0t,x} + \tfrac{1}{2}w_{t,x}^2\right)w_{t,xx} - b\tau w_{t,x} + b(\alpha/\beta + d_t/2)\tau_{,x} - (b/\beta)(w_t - w_b) = 0 \tag{62}$$

$$-D_{11b}w_{b,xxxx} + A_{11b}\left(u_{0b,x} + \tfrac{1}{2}w_{b,x}^2\right)w_{b,xx} + b\tau w_{b,x} + b(c - \alpha/\beta + d_b/2)\tau_{,x} + (b/\beta)(w_t - w_b) = 0 \tag{63}$$

$$u_{0b} - u_{0b} - (c + d_t/2 - \theta/\beta)w_{t,x} - (\theta/\beta + d_b/2)w_{b,x} - \left(\alpha\theta/\beta - c^3/6E_c\right)\tau_{,xx} + \delta\tau = 0 \tag{64}$$

were $\theta = c[c/(2E_c) + 1/k_t^v]$ and $\delta = c/G_c + 1/k_t^h + 1/k_b^h$.

Notice that the first two equations of the preceding system are the same as in Ref. 15, whereas the remaining three equations differ from their counterparts for the full bonded panel. In a limiting case when the spring coefficients approach infinity, the governing equations reduce to those in Ref. 15.

The boundary conditions for the ordinary edge [see Eqs. (30–33)] in terms of the unknowns are given at the face sheets by ($i = t, b$)

$$\xi A_{11i}\left(u_{0i,x} + w_{i,x}^2/2\right) = N_i \quad \text{or} \quad u_{0i} = \bar{u}_{0i} \tag{65}$$

$$\xi D_{11i}w_{i,xx} = M_i \quad \text{or} \quad w_{i,x} = \bar{w}_{i,x} \tag{66}$$

$$\xi\left[-D_{11i}w_{i,xxx} + A_{11i}\left(u_{0i,x} + w_{i,x}^2/2\right)w_{i,x} + (bd_i/2)\tau - m_i\right] = P_i \quad \text{or} \quad w_i = \bar{w}_i \tag{67}$$

and at any point through the height of the core by $\tau = 0$ or the fulfillment of either of the two conditions

$$\left(\alpha\theta/\beta - c^3/6E_c\right)\tau_{,x}(x) + (\theta/\beta)[w_b(x) - w_t(x)] + w_t(x)c = \bar{w}_c c \quad \text{or} \quad w_c(x, z_c) = \bar{w}_c(x, z_c) \tag{68}$$

where the last equality has been determined by substitution of Eq. (55) into Eq. (33).

In the case of an edge beam, the boundary equations Eqs. (37–39) are expressed in terms of the unknowns as

$$\xi\left[A_{11t}\left(u_{0t,x} + w_{t,x}^2/2\right) + A_{11b}\left(u_{0b,x} + w_{b,x}^2/2\right)\right] = N_G \quad \text{or} \quad u_A = u_G \tag{69}$$

$$\xi\left[A_{11t}\left(u_{0t,x} + w_{t,x}^2/2\right)z_t - A_{11b}\left(u_{0b,x} + w_{b,x}^2/2\right)z_b + D_{11t}w_{t,xx} + D_{11b}w_{b,xx}\right] = M_G \quad \text{or} \quad w_{A,x} = w_{G,x} \tag{70}$$

$$\xi\left[-D_{11t}w_{t,xxx} + A_{11t}\left(u_{0t,x} + w_{t,x}^2/2\right)w_{t,x} - D_{11b}w_{b,xxx} + A_{11b}\left(u_{0b,x} + w_{b,x}^2/2\right)w_{b,x} + b(z_t + z_b)\tau\right] = P_G \quad \text{or} \quad w_A = w_G \tag{71}$$

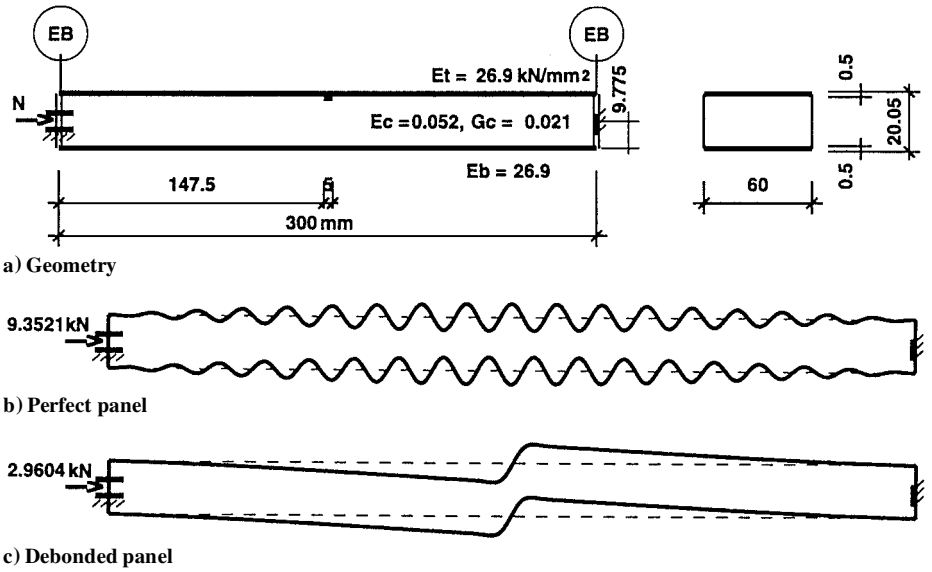

Fig. 5 Buckling modes of a sandwich panel with thin face sheets and short inner delamination centered at midspan.

Furthermore, Eqs. (44–46) of the continuity conditions at the face sheets in terms of the unknowns are written as

$$A_{11i}\left(u_{0i,x}^{(-)} - u_{0i,x}^{(+)}\right) = N_{ij} \tag{72}$$

$$D_{11i}\left(w_{i,xx}^{(-)} - w_{i,xx}^{(+)}\right) = M_{ij} \tag{73}$$

$$D_{11i}\left(w_{i,xxx}^{(+)} - w_{i,xxx}^{(-)}\right) + N_{ij}w_{i,x}(x = x_j) + \left(b^{(-)}d_i^{(-)} - b^{(+)}d_i^{(+)}\right)\tau(x = x_j)/2 - m_i^{(-)} + m_i^{(+)} = P_{ij} \tag{74}$$

Finally, the two sides of Eq. (48) are integrated and yield the following continuity condition in the core at $x = x_j$:

$$\left[\frac{\alpha^{(-)}\theta^{(-)}}{\beta^{(-)}} - \frac{c^2}{6E_c}\right]\tau_{,x}^{(-)} + \frac{\theta^{(-)}}{\beta^{(-)}}\left[w_b^{(-)} - w_t^{(-)}\right] + w_t^{(-)} = \left[\frac{\alpha^{(+)}\theta^{(+)}}{\beta^{(+)}} - \frac{c^2}{6E_c}\right]\tau_{,x}^{(+)} + \frac{\theta^{(+)}}{\beta^{(+)}}\left[w_b^{(+)} - w_t^{(+)}\right] + w_t^{(+)} \tag{75}$$

Notice that, when the spring coefficients left and right of $x = x_j$ are identical, Eq. (75) reduces to

$$\tau_{,x}^{(-)} = \tau_{,x}^{(+)} \tag{76}$$

by virtue of Eq. (42).

The finite difference discretization of the formulation, as well as the numerical solution procedure, follows the outline presented in Ref. 19.

III. Numerical Study

Buckling of sandwich panels with inner and edge debondings (delaminations) that are located at the upper face sheet–core interface is discussed. The inner delamination does not extend to the ends of the panel, whereas the edge delamination starts at one of the panel edges (Fig. 1a). The compressive in-plane loads are applied either directly to the face sheets of the panel or through a rigid edge beam connecting the two face sheets. The influence of the main factors, such as location and length of the debonded region, rigidities of the face sheets and core, contact between the debonded face sheet and core layer, as well as boundary conditions on the buckling behavior of sandwich panels, is examined. Three basic cases are discussed. The first two cases represent the debonded sandwich panels with and without contact between the debonded face sheet and core. The third case, which is referred to as the perfect panel, represents the full bonded sandwich panel.

A note should be made concerning the treatment of the case without contact. It is implied in this case that the peeling stresses between the debonded face sheet and the core do not exist through the predetermined delamination. As has been mentioned in the preceding section, this situation is resolved by setting the value of the vertical spring coefficient in the delaminated region to a very low value (in addition to a very low value of the horizontal spring coefficient used for the case with contact). Therefore, in the computed buckling mode, either the face sheets must have the identical vertical displacements through the delaminated region or they must move away of each other; otherwise, the solution is discarded.

A. Inner Debonding (Delamination)

The sandwich panel with thin face sheets and short debonded region located symmetrically about midspan appears in Fig. 5a. The in-plane loads are applied to the sandwich panel through edge beams that globally clamp the panel edges. The perfect panel buckles into a wrinkling mode that is symmetric about midspan and consists of 35 sinusoidal half-waves with nonuniform amplitudes at each face sheet (Fig. 5b). The introduction of the delamination only 5 mm long leads to a drastic change in the buckling response; the critical load reduces by about 70% as compared with the perfect panel, whereas the corresponding buckling shape changes from the wrinkling local symmetric mode into a global localized antisymmetric mode (Fig. 5c). Here the antisymmetry is about midspan and midheight of the panel. The displacement pattern is nearly linear up to the tips of the debonded zone, whereas the pronounced nonlinearity takes place within the debonded region. The displacements of the two face sheets are identical along the entire length of the panel including the debonded zone. Thus, the existence or inexistence of contact between the debonded face sheet and core does not affect the response.

An eightfold increase in the debonded length (to 40 mm long; Fig. 6a) for the sandwich panel from the preceding example brings about a qualitative change in its buckling response; the buckling mode has changed from the global localized antisymmetric response (Fig. 5c) into a localized symmetric mode for the case without contact (Fig. 6b) and into a localized antisymmetric mode for the case with contact (Fig. 6c). In both cases the buckling modes are symmetric about midspan, whereas the first pattern is symmetric about midheight of the panel and the second one is antisymmetric. The critical loads of the delaminated panels are about only 6–7% of that for the perfect panel, and there is a drastic change in the buckling modes (see Figs. 6b and 6c).

The influence of the length l_d of inner delamination centered at midspan on the critical buckling loads of the debonded sandwich panel with thin face sheets and the edge beams appears in Fig. 7. The

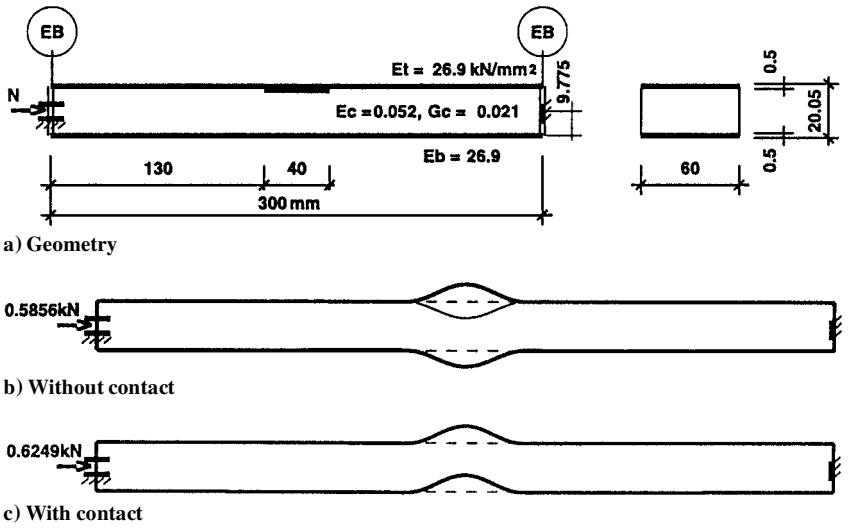

Fig. 6 Buckling modes of a sandwich panel with thin face sheets and long inner delamination centered at midspan.

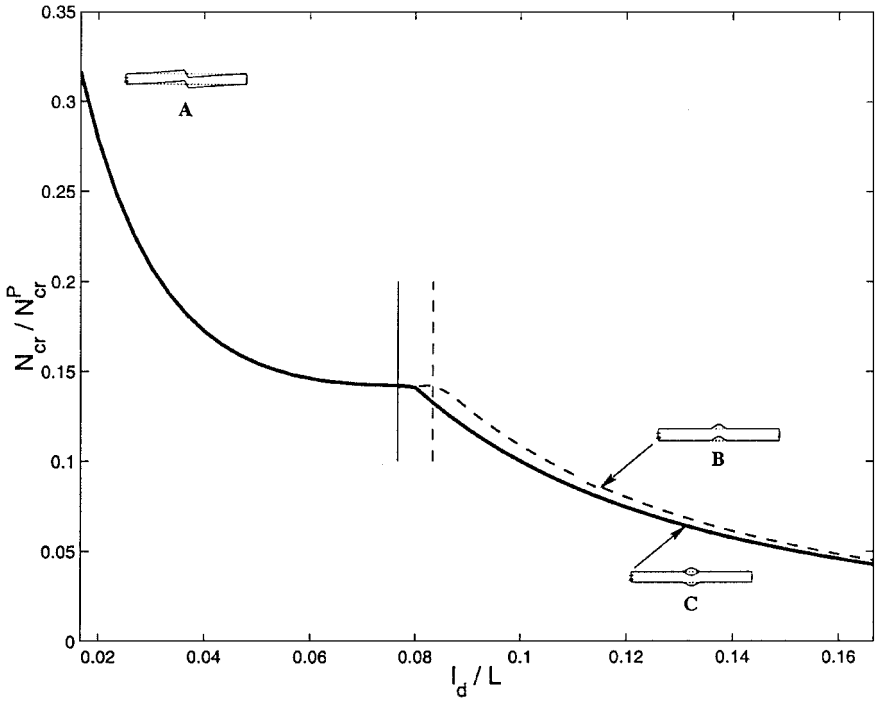

Fig. 7 Effect of the length of an inner delamination centered at midspan on the critical loads of sandwich panel with thin (0.5-mm) face sheets: ——, without contact, and – – –, with contact.

results reveal that the ratio between the critical loads of the debonded and the perfect panels, N_{cr}/N^P_{cr}, reduces with the increase in debonding length. However, for the medium-sized delaminations, the reduction rate essentially decreases. Moreover, for the contact case the local maximum is determined at the debond length of 26 mm, after which the global localized antisymmetric mode (Fig. 7, case A) shifts into the localized antisymmetric mode (Fig. 7, case B). In the absence of contact the shift from case A to the localized symmetric mode (Fig. 7, case C) occurs after the length of debond exceeds 24 mm, but the local maximum does not exist in this case.

Figure 8 presents the effect of location L_d of a delamination 10 mm long on the buckling response of a panel with thin face sheets. The location of the delamination along the span of the panel is defined by the distance of its center from the left end of the panel. Notice that there is a position where the critical buckling load reaches its minimum. This happens in both cases, with and without contact, when the center of debond is at a distance of 16 mm from the left end of the panel (Fig. 8, point b). However, the buckling response (the global localized antisymmetric mode) remains the same at all locations (Fig. 8, points a, b, and c).

The next two examples consider sandwich panels with thick and very thick face sheets and short inner delaminations 10 mm long. The perfect panel with thick face sheets (Fig. 9a) buckles into a global symmetric mode (Fig. 9b), whereas the delaminated panel exhibits a global antisymmetric buckling behavior (Fig. 9c). The critical load level of the delaminated panel is reduced by about 3.5% only, which suggests that the increase in the rigidity of the face sheets minimizes the effect of delamination. Moreover, when the thickness of the face sheets increases to 3.5 mm (Fig. 10a), the buckling modes of the perfect and delaminated panels are similar global symmetric modes (Figs. 10b and 10c), and the values of the critical loads are practically identical. Here, as in the case of the panels with thin face sheets and short inner delamination, the displacements of the two face sheets are identical along the span of the panels, and therefore, the existence or inexistence of contact at the delamination zone does not affect the response.

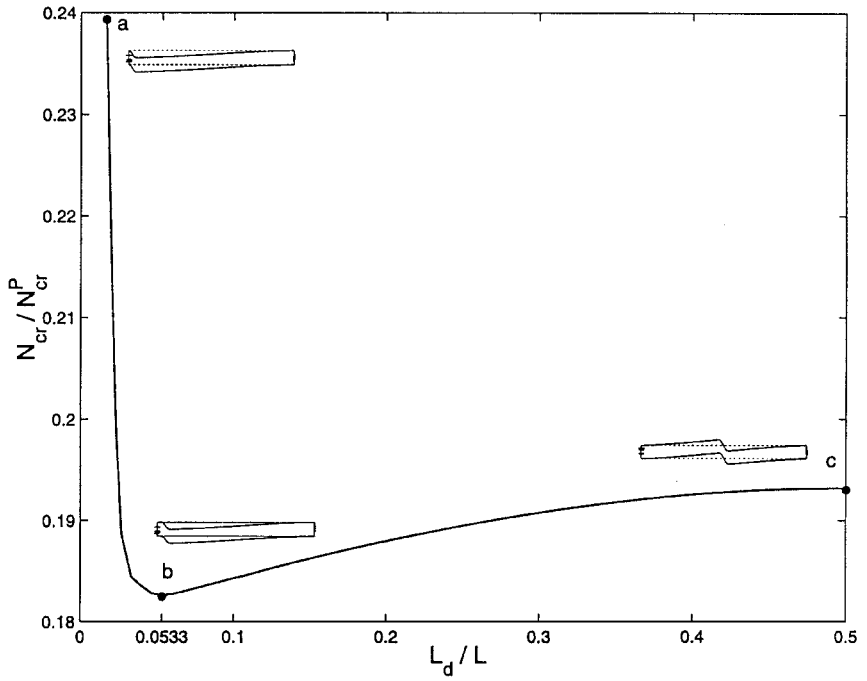

Fig. 8 Effect of the location of the delamination zone of 10 mm long on the critical loads of sandwich panel with thin (0.5-mm) face sheets.

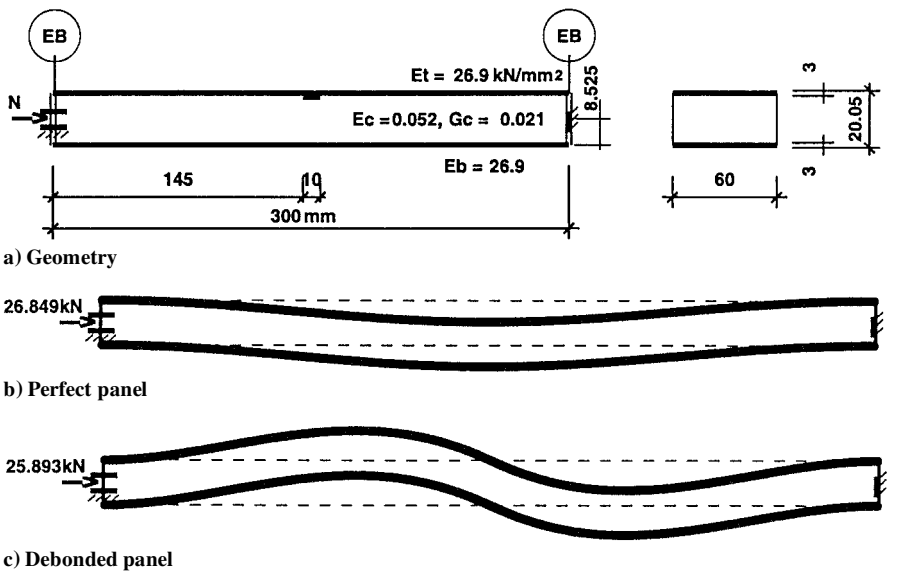

Fig. 9 Buckling modes of a sandwich panel with thick face sheets and short inner delamination centered at midspan.

The effects of the length of inner delamination with and without contact that is centered at midspan on the buckling response of the debonded sandwich panels with thick (3-mm) and very thick (3.5-mm) face sheets appear in Fig. 11. The global symmetric mode (case A in Fig. 11), for both types of panels, shifts into the global antisymmetric mode (case B) at the delamination length 8 and 15 mm long for the panels with thick and very thick faces, respectively, regardless of the existence of contact in the debonded region. Moreover, the horizontal portions of the curves in Fig. 11 reveal that up to these values the presence of delamination does not affect the buckling response of the panels.

Figure 12 presents the effects of location of short (10-mm-long) delamination on the buckling response of the sandwich panels with thick and very thick face sheets. As in the case of thin face sheets (Fig. 8), the curves exhibit global minima (see points b in Fig. 12) corresponding to the debond locations, which result in the lowest buckling loads of the debonded panels. The minimum buckling loads occur at a distance of 62 and 66 mm between the center of delamination and the left end of the panel for the panels with thick and very thick face sheets, respectively, in either case, with or without contact (Fig. 12, points b). In addition, for the panels with thick face sheets, the global symmetric mode corresponding to the leftmost position of the debond (Fig. 12, point a) transforms gradually, through the asymmetric global modes (point b), into the antisymmetric pattern of point c. On the other hand, the starting global symmetric buckling shape of the panel with very thick face sheets (Fig. 12, point a) is violated for the intermediate locations of the delamination (point b), as in the case of the thick face sheets, but the global symmetry is then restored for the central position of the delamination (point c).

The effects of rigidity of the face sheets on the buckling behavior of delaminated panels with short and long inner delaminations appear in Figs. 13 and 14, respectively. When the delamination centered at midspan is 10 mm long, the global localized antisymmetric buckling mode (Fig. 13, case A) corresponding to the thin face sheets (0.5 mm) gradually transforms into the global antisymmetric buckling mode (case B) with an increase in the thickness of the face

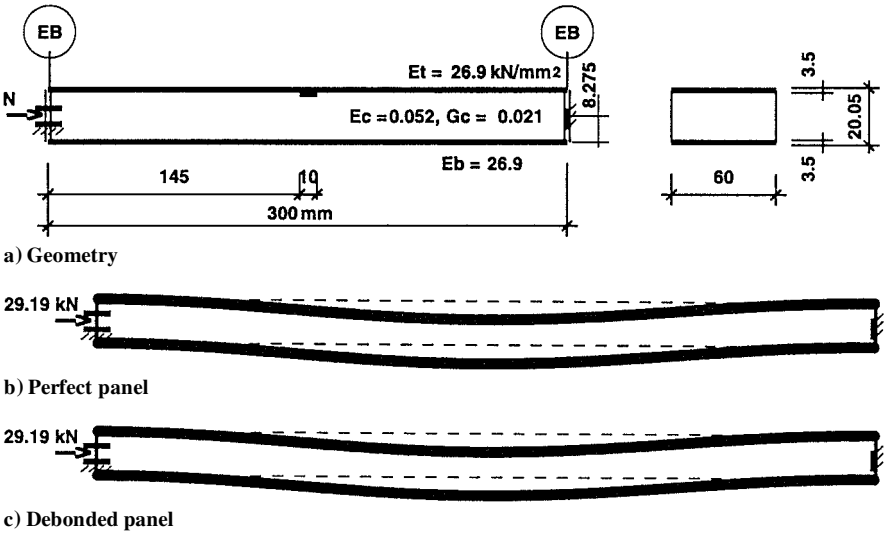

Fig. 10 Buckling modes of a sandwich panel with very thick face sheets and short inner delamination centered at midspan.

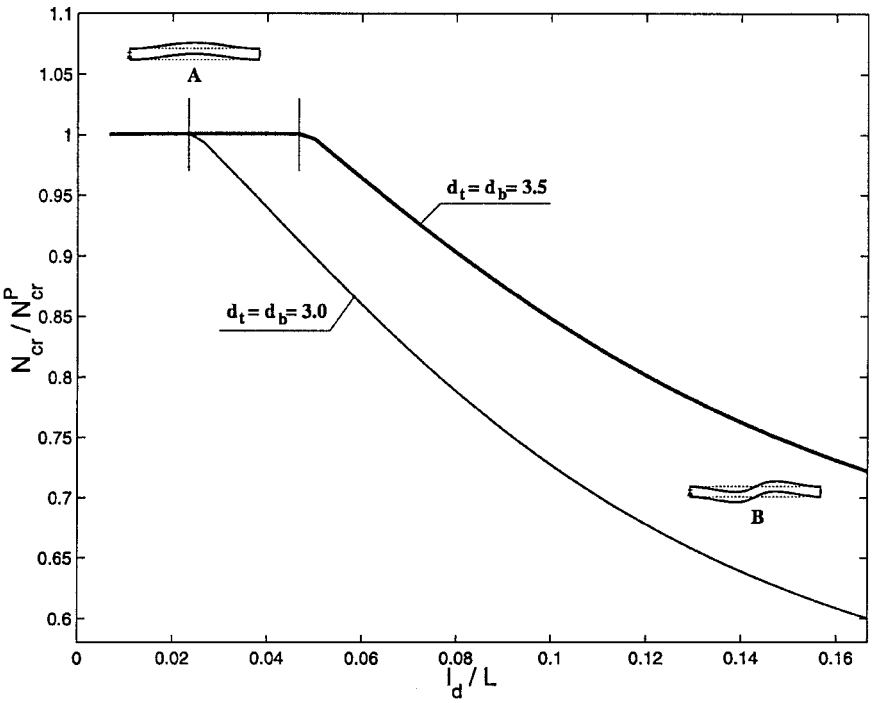

Fig. 11 Effect of the length of an inner delamination centered at midspan on the critical loads of sandwich panels with thick (3-mm) and very thick (3.5-mm) face sheets.

sheets. At a thickness of 3.3 mm, the global antisymmetric mode shifts into a global symmetric mode (case C) that yields the sudden change in the curve at this point. The other break in the curve occurs at a thickness of 0.8 mm, where the wrinkling mode of the perfect panel (see Fig. 5b) is changed into the global symmetric buckling pattern.

If the delamination length is increased to 40 mm, the localized modes (Fig. 14, cases A and B) corresponding to the panels with thin face sheets shift to the global localized antisymmetric mode (case C) at a thickness of 0.8 mm in the case with contact and at a thickness of 0.9 mm for the case without contact, respectively. The broken line reflecting these shifts (and the shift in the buckling mode of the perfect panel mentioned earlier) is given on an enlarged scale in Fig. 14. A further increase in the thickness of face sheets leads to a gradual transformation of the global localized antisymmetric mode into the global antisymmetric one (Fig. 14, case D).

Notice that the buckling modes determined numerically on the basis of the HSAPT and presented in Figs. 5c, 6b, 9c, and 10c have been observed in the Avery et al.[9] experimental study.

In addition to the pure buckling modes that have been observed up to this point, sandwich panels may exhibit modes that consist of interaction between the different patterns presented before. Figure 15 presents the results for a sandwich panel with thin clamped face sheets, where the edges of the core are free of shear traction. The mechanical properties of the core in this case have been increased by an order of magnitude relative to the earlier examples. The delamination considered is 38 mm long, located at the upper face sheet–core interface, and centered at midspan of the panel. The resulting interactive mode buckling response, which consists of an interaction between the global localized antisymmetric mode (Fig. 5c) and the localized symmetric mode (Fig. 6b), appears in Fig. 15b. The vertical displacement patterns of the face sheets (w_t and w_b), denoted by W in Fig. 15c, reveal that the two face sheets have identical displacements up to the tips of the delaminated zone. Within the delaminated zone, the face sheets move symmetrically about the line connecting the tips of the zone. The ends of the face sheets are fixed only locally, which does not provide the full fixity to the panel edge as a whole, and therefore, the edges of

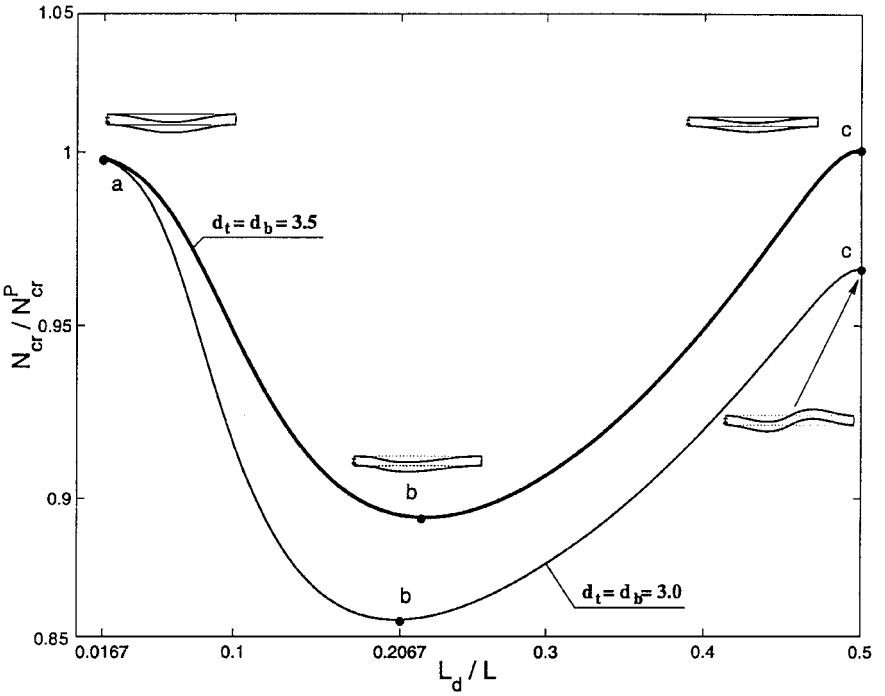

Fig. 12 Effect of the location of the delamination zone of length 10 mm on the critical loads of sandwich panels with thick (3-mm) and very thick (3.5-mm) face sheets.

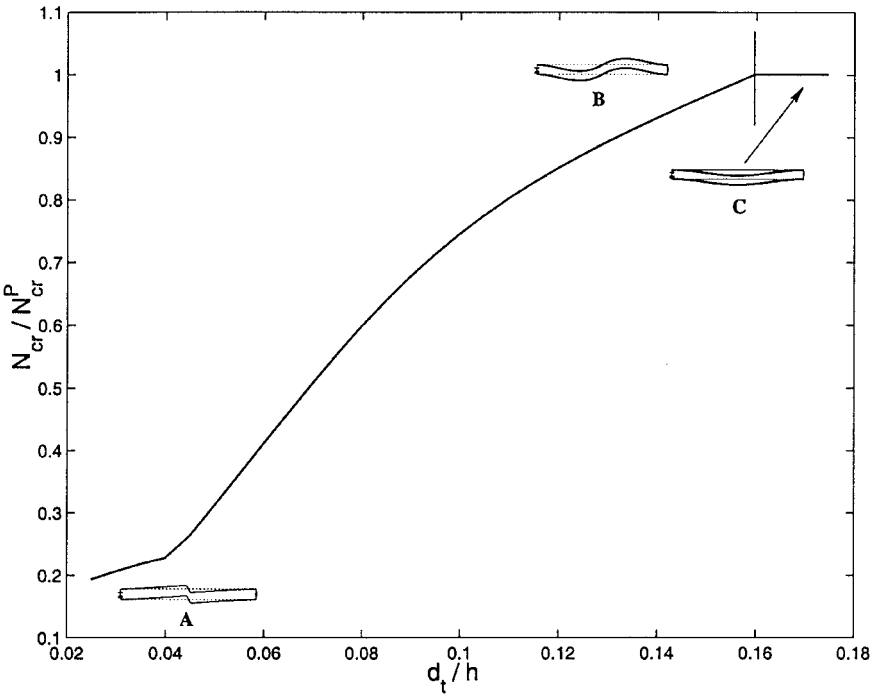

Fig. 13 Influence of the thickness of the face sheets on the critical loads of sandwich panel with short (10-mm) inner delamination centered at midspan.

the panel may rotate globally. The longitudinal displacements (u_t and u_b), denoted by U in Fig. 15c, follow a global asymmetrical pattern. The shear stresses τ exhibit abrupt changes at the tips of the delaminated zone and disappear within the debonded region.

B. Edge Debonding (Delamination)

The effect of the edge delamination on the buckling of a sandwich panel with thin face sheets is examined. The panel is simply supported only at its lower face sheet and is free at its upper face sheet. In addition, the core edges are free of shear traction (Fig. 16a). The delamination zone originates at the left edge of the upper face sheet–core interface and extends to 10 mm into the span of the panel. The perfect panel exhibits a localized buckling mode with displacements confined to the vicinity of the panel edges (Fig. 16b). The delaminated panel buckles into a localized buckling mode limited mainly to the delaminated zone (Figs. 16c and 16d). For the case without contact, the critical buckling load is about 9% of that for the perfect panel. This load level is equal to the Euler buckling load of a cantilever beam with the cross section identical to that of the face sheet and the span corresponding to the debond length. The last observation is shown in Fig. 16c, where the upper face sheet and core break away. If contact exists within the delamination zone, the upper face sheet and core move together (Figs. 16d), and the critical buckling load is larger by about 19% as compared to the case without contact.

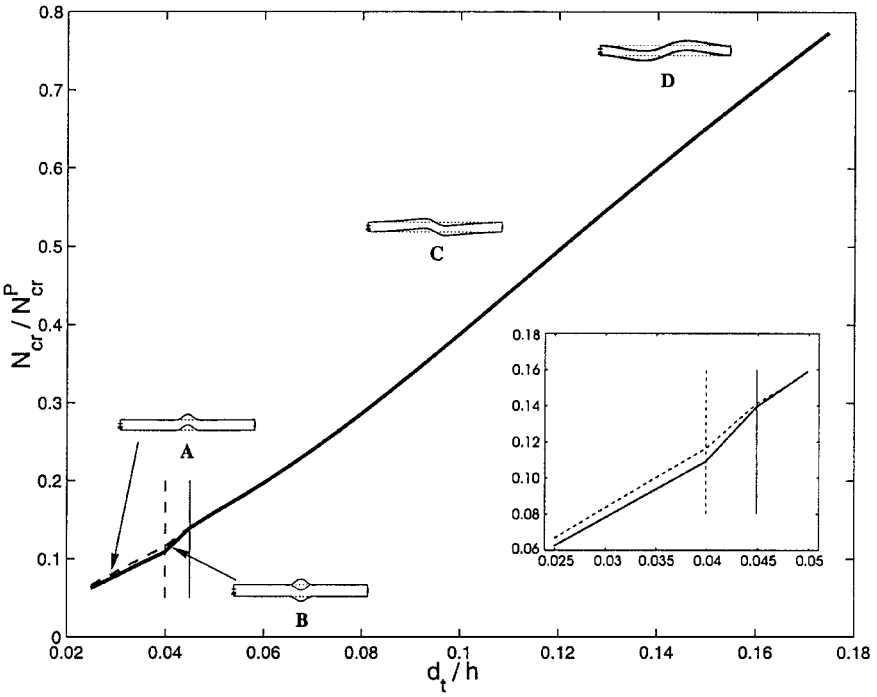

Fig. 14 Influence of the thickness of the face sheets on the critical loads of sandwich panel with long (40-mm) inner delamination centered at midspan: ——, without contact, and – – –, with contact.

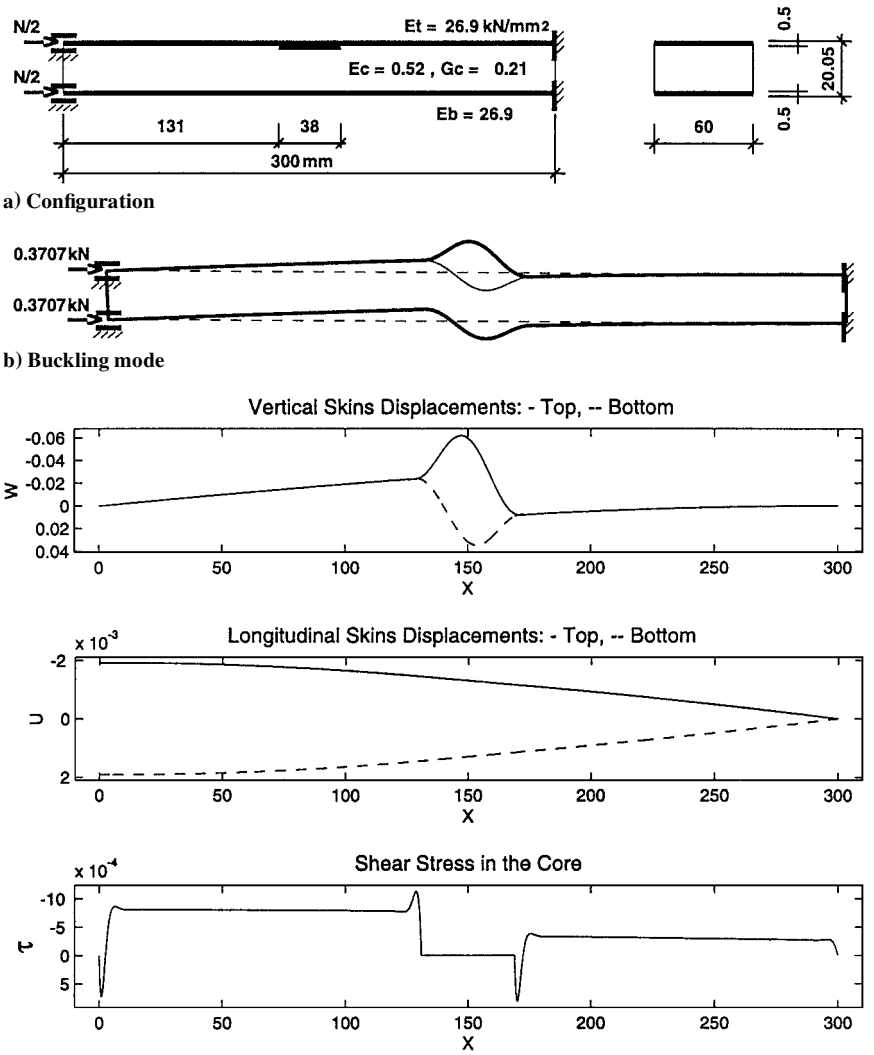

a) Configuration

b) Buckling mode

c) Displacement and stress diagrams

Fig. 15 Locally clamped debonded sandwich panel with thin face sheets and long inner delamination at midspan.

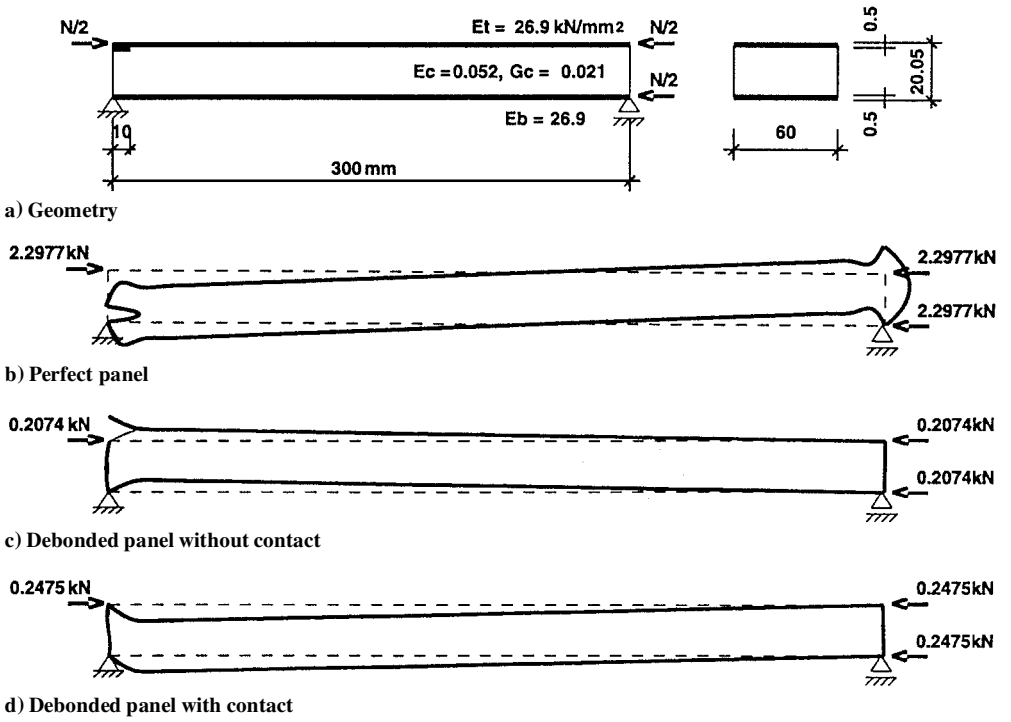

Fig. 16 Buckling modes of a sandwich panel with thin face sheets and short edge delamination.

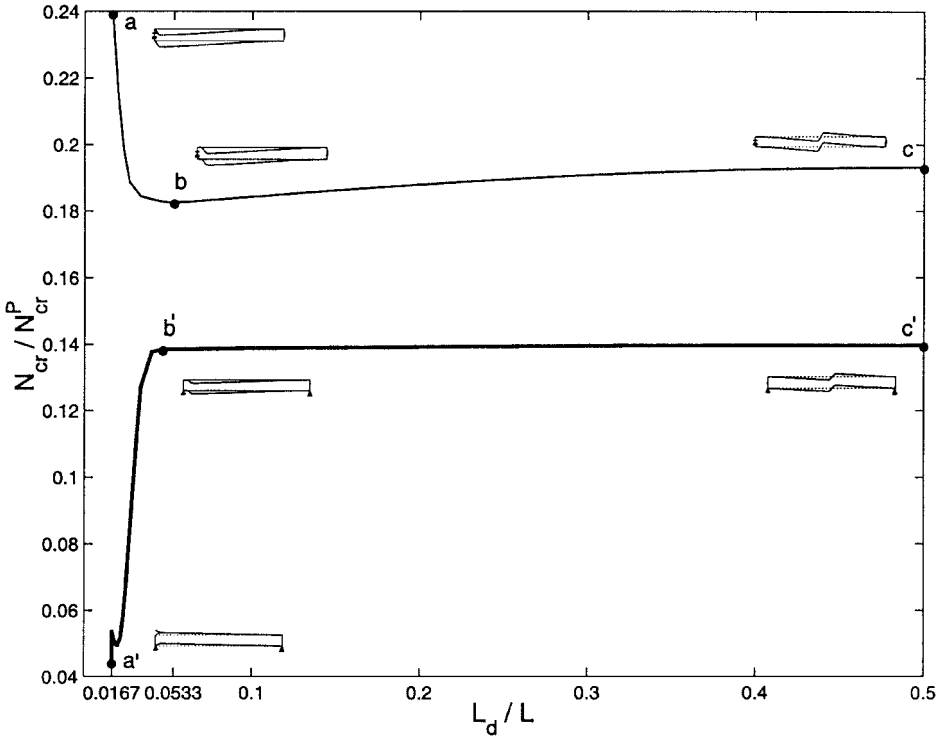

Fig. 17 Effect of the location of the delamination zone 10 mm long on the critical loads of a sandwich panel with thin (0.5-mm) face sheets simply supported at its lower face sheet only (bold line) in comparison with Fig. 8 (thin line).

Figure 17 presents the effects of location of a short delamination 10 mm long on the critical loads of the panel discussed in Fig. 16a in comparison with the results for the panel with edge beams from Fig. 8. The buckling loads in both cases are normalized with respect to the critical buckling load of the perfect panel with edge beams. Notice that the panel considered in this case differs from the panel with edge beams by the boundary conditions. Here the upper face sheet, as well as the core edges, are free of stresses, and the panel is simply supported only at its lower face sheet. The results reveal that a drastic difference between the cases with and without contact occurs only for the leftmost position of the delamination, that is, in the case of the edge delamination (see Fig. 16c and point a′ in Fig. 17). For the other locations of the debond, where it becomes an inner delamination, the difference between the cases with and without contact is immaterial. Notice that the abrupt increase in the buckling load at the point immediately following point a′ is the consequence of the qualitative change in the character of the delamination. Namely, point a′ reflects the edge delamination whereas any other point reflects the inner delamination, even though it can be offset as small as one likes from the panel edge. The local minimum

occurs at a distance of 6 mm from the left end of the panel to the center of delamination (see bold line in Fig. 17). The localized pattern that is confined to the support zone (Fig. 17, points a′ and b′) gradually transforms to the global localized antisymmetric mode (point c′) when the delamination location moves from the edge to the center of the panel. A comparison between the critical loads of the simply supported panel and those of the panel with edge beams (thin line in Fig. 17) reveals that the global fixing of the panel edges provided by edge beams is most efficient when the debond is located at the vicinity of the support. When the distance of the debond from the left end of the panel is greater than 10 mm, the effect of clamping is reduced, but still a significant difference remains between the critical loads in the range from 32% at point b′ to 38% at point c′.

IV. Conclusions

A linear buckling analysis of the debonded (delaminated) sandwich panels with a transversely flexible core has been presented. The analysis is based on the principles of HSAPT[15] and allows for the nonrigid bond layers, modeled by equivalent horizontal (shear) and vertical (contact) springs, between the face sheet and core. The debonding is simulated through a reduction of the spring coefficients to values approaching zero. The effects of location and length of the debonded region, rigidities of the face sheets, boundary conditions, as well as of contact between the debonded face sheet and core on the buckling behavior of sandwich panels have been investigated for some typical panels.

The influence of an inner delamination on the buckling response of the sandwich panels with thin face sheets is quite severe; the critical buckling loads are reduced to about 5–30%, and the corresponding buckling modes exhibit a drastic change with respect to those without delamination. Moreover, an increase in the debonding length leads to a shift in the buckling response from the global localized antisymmetric mode to the localized symmetric one. The influence of the inner delamination on the critical load level of the sandwich panels with thick face sheets is minor, although the buckling modes may shift from the global symmetric pattern into the global antisymmetric one. It has also been revealed that the short inner delamination, placed at midspan of the panel with very thick face sheets, has no influence on its buckling behavior.

It has been shown that, for all configurations considered, there are delamination locations for which the buckling resistance of the panel is the lowest. It has also been observed that an increase in the face sheet stiffnesses leads to an increase in the critical buckling loads, as well as to shifts in the buckling modes for both bonded and debonded panels. In general, the effect of contact is minor, except for the cases of long inner and edge delaminations.

The global clamping of the sandwich panel by the edge beams is advantageous over the simply supported edge, when the delamination zone is located near the support; for the other locations, the difference between the buckling loads diminishes but still remains significant (about 32–38%).

The local fixing of the delaminated sandwich panel with thin face sheets at its edges leads to an interactive mode buckling response that consists of a combination of the basic patterns such as the global localized antisymmetric mode and the localized symmetric mode.

The edge delamination has been found to be a very dangerous type of an imperfection that sandwich panel cannot sustain. Thus, special precautions must be taken to prevent such imperfection either during manufacturing process or during service life of the sandwich panel.

A comparison with the experimental study of Avery et al.[9] reveals that the numerical simulation of the buckling response is in a qualitative agreement with the test results. The present formulation enhances the physical understanding of the phenomena involved and provides a thorough insight into the role of the main response parameters. Further research in this field along the lines and principles of the HSAPT outlined in this paper is the challenge that the sandwich panel industry must consider to achieve a confident design.

References

[1]Kassapoglou, C., "Buckling, Post-Buckling and Failure of Elliptical Delaminations in Laminates Under Compression," *Composite Structures*, Vol. 9, No. 2, 1988, pp. 139–159.

[2]Somers, M., Weller, T., and Abramovich, H., "Influence of Predetermined Delaminations on Buckling and Postbuckling Behavior of Composite Sandwich Beams," *Composite Structures*, Vol. 17, No. 4, 1991, pp. 295–329.

[3]Hwu, C., and Hu, J. S., "Buckling and Postbuckling of Delaminated Composite Sandwich Beams," *AIAA Journal*, Vol. 30, No. 7, 1992, pp. 1901–1909.

[4]Simitses, G. J., Sallam, S., and Yin, W. L., "Effect of Delamination of Axially Loaded Homogeneous Laminated Plates," *AIAA Journal*, Vol. 23, No. 9, 1985, pp. 1437–1444.

[5]Kim, W. C., and Dharan, C. K. H., "Facesheet Debonding Criteria for Composite Sandwich Panels Under In-Plane Compression," *Engineering Fracture Mechanics*, Vol. 42, No. 4, 1992, pp. 643–652.

[6]Lin, C. C., Cheng, S. H., and Wang, J. T. S., "Local Buckling of Delaminated Composite Sandwich Plates," *AIAA Journal*, Vol. 34, No. 10, 1996, pp. 2176–2183.

[7]Kardomateas, G. A., "Growth of Face-Sheet Delaminations in Sandwich Beams Under Compression or Bending," *Recent Advances in Mechanics of Aerospace Structures and Materials*, edited by B. V. Sankar, Vol. 56, American Society of Mechanical Engineers, New York, 1998, pp. 173–180.

[8]Zenkert, D., "Strength of Sandwich Beams with Interface Debondings," *Composite Structures*, Vol. 17, No. 4, 1991, pp. 331–350.

[9]Avery, J. L., Manickam, N., and Sankar, B. V., "Compressive Failure of Debonded Sandwich Beams," *Recent Advances in Mechanics of Aerospace Structures and Materials*, edited by B. V. Sankar, Vol. 56, American Society of Mechanical Engineers, New York, 1998, pp. 207–217.

[10]Plantema, F. J., *Sandwich Construction*, Wiley, New York, 1966, Chaps. 2 and 3.

[11]Allen, H. G., *Analysis and Design of Structural Sandwich Panels*, Pergamon, London, 1969, Chaps. 2 and 9.

[12]Zenkert, D., *An Introduction to Sandwich Construction*, Chameleon, London, 1995, Chap. 1.

[13]Noor, A. K., Burton, W. S., and Bert, C. W., "Computational Models for Sandwich Panels and Shells," *Applied Mechanics Review*, Vol. 49, No. 3, 1996, pp. 155–199.

[14]Frostig, Y., Baruch, M., Vilnay, O., and Sheinman, I., "High-Order Theory for Sandwich-Beam Behavior with Transversely Flexible Core," *Journal of Engineering Mechanics*, Vol. 118, No. 5, 1992, pp. 1026–1043.

[15]Frostig, Y., and Baruch, M., "High-Order Buckling Analysis of Sandwich Beams with Transversely Flexible Core," *Journal of Engineering Mechanics*, Vol. 119, No. 3, 1993, pp. 476–495.

[16]Brush, D. O., and Almroth, B. O., *Buckling of Bars, Plates, and Shells*, McGraw–Hill, New York, 1975, Chaps. 1–3.

[17]Thomsen, O. T., and Frostig, Y., "Localized Bending Effects in Sandwich Panels: Photoelastic Investigation Versus High-Order Sandwich Theory Results," *Composite Structures*, Vol. 37, No. 1, 1997, pp. 97–108.

[18]Frostig, Y., "Behavior of Delaminated Sandwich Beams with Transversely Flexible Core—High Order Theory," *Composite Structures*, Vol. 20, No. 1, 1992, pp. 1–16.

[19]Sokolinsky, V., and Frostig, Y., "Boundary Condition Effects in Buckling of Soft Core Sandwich Panels," *Journal of Engineering Mechanics*, Vol. 125, No. 8, 1999, pp. 865–874.

[20]Sokolinsky, V., and Frostig, Y., "Branching Behavior in the Nonlinear Response of Sandwich Panels with a Transversely Flexible Core," *International Journal of Solids and Structures*, Vol. 37, No. 40, 2000, pp. 5745–5772.

[21]Whitney, J. M., *Structural Analysis of Laminated Anisotropic Plates*, Technomic, Lancaster, PA, 1987, Chaps. 1 and 2.

A. M. Waas
Associate Editor